Sigma J Eng & Nat Sci 38 (3), 2020, 1217-1233

Sigma Journal of Engineering and Natural Sciences
Sigma Mühendislik ve Fen Bilimleri Dergisi

Research Article

CHROMIUM (Cr(VI)) REMOVAL FROM WATER WITH BENTONITE-MAGNETITE NANOCOMPOSITE USING RESPONSE SURFACE METHODOLOGY (RSM)

Pınar BELİBAĞLI[1], Buşra Nur ÇİFTCİ[2], Yağmur UYSAL*[3]

[1]*Department of Environmental Engineering, Mersin University, MERSİN;* ORCID: 0000-0001-6643-9620
[2]*Department of Environmental Engineering, Mersin University, MERSİN;* ORCID: 0000-0003-3674-0580
[3]*Department of Environmental Engineering, Mersin University, MERSİN;* ORCID: 0000-0002-7217-8217

Received: 26.05.2020 Revised: 13.06.2020 Accepted: 30.06.2020

ABSTRACT

In this study, magnetite nanocomposites coated with bentonite were synthesized as adsorbent material and their effects in Cr (VI) adsorption were investigated. Magnetite nanomaterials (Bentonite-Fe_3O_4) were characterized by surface morphology (SEM-EDX) and elemental analyses (FTIR). RSM was used to investigate the optimum ambient conditions of parameters for the removal of Cr (VI) ions. Isotherm and kinetic models were calculated to determine the mechanism of adsorption, and obtained results showed that Cr (VI) adsorption by Bentonite-Fe_3O_4 was more suitable for Tempkin isotherm (R^2:0.99) and second-order kinetic model (R^2:1). The optimum adsorption efficiency (77.46%) of Cr (VI) ions in 6.5 mg/L concentration was obtained at contact time of 60 min, pH 2.0, adsorbent dosage of 2.5 g/L and at 35 ^oC.
Keywords: Adsorption, bentonite, chromium, nanomagnetite, response surface methodology.

* Corresponding Author: e-mail: yuysal@mersin.edu.tr, tel: (324) 361 00 01 / 17092

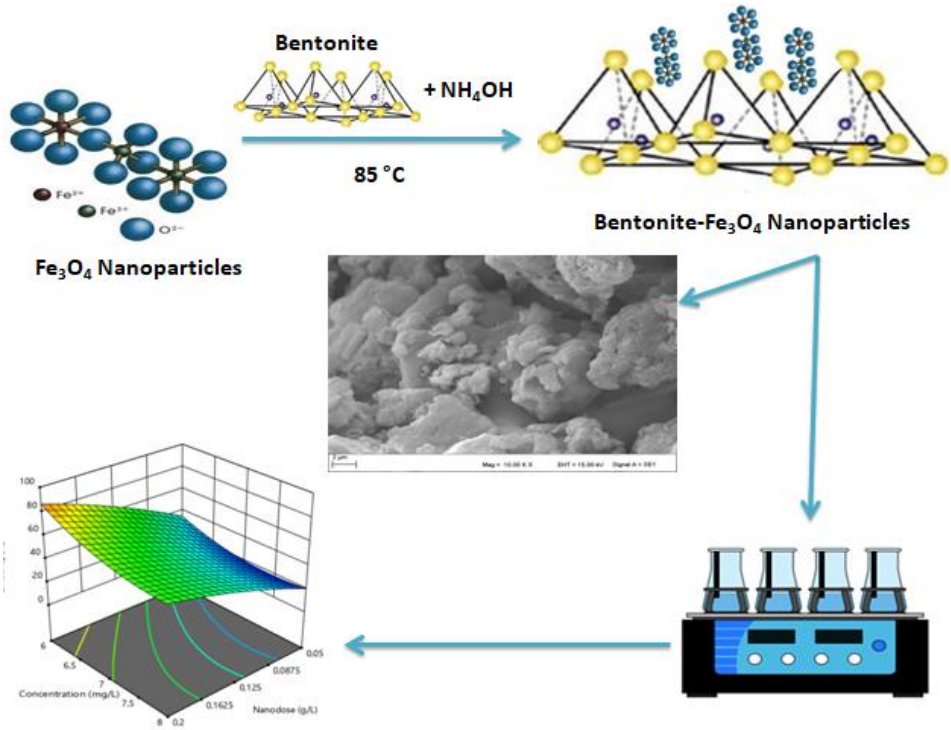

1. INTRODUCTION

Industrial and domestic wastewater discharges containing heavy metal ions impair the quality of surface and groundwater, and cause serious dam age to the water ecosystem and its flora-fauna. [1]. Heavy metals are highly soluble in water and easily transferred to the food chain, so they pose a serious threat to humans, animals and plants [2-5]. Great efforts are made to remove these compounds from water systems due to their non-degradable, highly toxic, permanent properties [6, 7]. Highly toxic and commonly used heavy metal ions by industries are chromium (Cr), cadmium (Cd), arsenic (As), lead (Pb) and mercury (Hg) [8]. Chromium are mainly found as either mobile and highly toxic Cr (VI) anions or insoluble Cr (III) hydroxide residues in water. [9]. Hexavalent chromium can cause many diseases such as cancer and liver damage in mammals. For this reason, it is important to remove Cr (VI) from wastewater before discharge to nature [10]. The removal of chromium ions from water is usually carried out by methods such as biological treatment, coagulation, adsorption and chemical reduction [11].

Adsorption is one of the techniques used to eliminate heavy metal ions from solutions due to its cheap cost, environmental kindness, and high performance [12]. A good adsorbent should supply adequate binding areas for suitable adsorption of metal ions [13, 14]. Nanomaterials have attracted attention in wastewater treatment due to their unique surface areas, low flocculant production and high active groups found for easy binding of metal ions [15, 16]. Recently, many nanomaterials are used as adsorbent due to their high pollutant removal efficiencies in wastewater treatment, such as graphene oxide, chitosan, clays, etc. In the last few years, clay minerals have attracted much interest because of their low cost, hydrophilicity and more active sites [17]. Bentonite is a type of clay which is abundant in nature, has low conductivity and cation exchange capacity and has a high specific surface area [18]. Based on these advantages, the application of

bentonite to adsorb heavy metal ions in wastewater has great research potential [19]. However, the difficulty of separating bentonite from wa ter limits its practical application. In recent years, magnetic materials such as Fe_3O_4, which can be easily separated from the solution using magnetic fields, have been extensively used in water treatment [20–23]. The small particle size, high surface area/volume ratio and superior magnetic property of Fe_3O_4 nanoparticles give them a fast and effective separation potential [24, 25]. The use of developed analytical systems and efficient optimization instruments is most expedient for experimental assessment and optimization of reaction models [26]. RSM is a program using statistical and numerical methods by optimizing theoretical and laboratory data with different independent variables [27, 28]. The Central Composite Design (CCD) method is one of the commonly used RSM's, and this method has proven to be an efficient technique for the working parameters in many applications, especially environmental implementation [29].

The main objective of this study is to investigate the Cr(VI) sorption potential of bentonite/magnetite (Fe_3O_4) composite synthesized as adsorbent material from an aqueous solution by using Response Surface Methodology (RSM). The novelty of this study is to obtain a new composite material from two materials, both of which have superior adsorption properties, and to combine these superior properties in a single substance. At the same time, the generation of high production costs by using only magnetite has been reduced by adding bentonite, which is abundant in nature. Although bentonite is a substance with high adsorption feature when used alone in its pure form, problems such as high dispersion in water and quite difficult to separate from water are eliminated when used with magnetite. Thus, adsorption experiments were carried out to determine this composite material on the sorption of Cr(VI) ions. The important factors affecting adsorption efficiencies such as solution pH, contact time, and initial Cr(VI) concentration were investigated. The Langmuir, Freundlich, Tempkin, and Scarthard isotherm models were also used to study the equilibrium of the adsorption process. The best kinetic and isotherm models were also found from experimental data.

2.2. MATERIAL AND METHODS

2.1. Synthesis of Bentonite-Magnetite Nanoparticles

The Bentonite-Fe_3O_4 nanoparticles were synthesized according to Petcharoen and Srivat [30]. Firstly, 6 g bentonite was dispersed in 300 mL of deionized water. Then a magnetite nanoparticle (Fe_3O_4) solution was prepared by adding 13.795 g $FeCl_3.6H_2O$ and 7.095 g $FeSO4.7H_2O$ into 300 mL of deionized water under N_2 medium. When the solution temperature reached 85 °C, 25 mL of 25% purity ammonia (NH_3) and bentonite solutions were added and stirred for 30 minutes to be a homogeneous mixture. During the reaction, black color was observed in the solution, and this color change was due to the formation of magnetite bentonite particles. The synthesized Bentonite-Fe_3O_4 particles were washed 4-5 times with deionized water and separated with a neodymium magnet.

2.2. Adsorption Studies

Batch adsorption studies were carried out in 100 mL flasks, and these flasks were mixed thoroughly using an orbital shaker at a constant speed. The optimum conditions were investigated to find out effective parameters for the removal of hexavalent chromium ions such as Bentonite-Fe_3O_4 dose, contact time and initial Cr (VI) concentrations of the solutions. After that, suspensions were centrifuged, and the concentrations of Cr (VI) in the supernatant solutions were analyzed using a spectrophotometer (Hach-Lange DR-3900). All adsorption studies were done in duplicate and mean values were reported. The Cr (VI) removal efficiency (%) was calculated according to Eq 1 and 2, as below:

$$qe = \frac{(C_0 - C_e)}{V} * M \quad (1)$$

$$\% = \frac{(C_0 - C_e)}{C_0} * 100 \quad (2)$$

Where; C_0 (mg/L); initial Cr (VI) concentration, C_e (mg/L); equilibrium Cr (VI) concentration, M(g); the mass of bentonite-Fe_3O_4, V (L); volume of the solutions, qe (mg/g); adsorption capacity of bentonite-Fe_3O_4 nanocomposite

2.3. RSM-CCD model

The experimental data was analyzed and fitted by RSM using Design Expert 12 software. RSM allows to find process optimization and possible effectiveness of all parameters with minimum experimental studies. The effect of different operating parameters such as bentonite-Fe_3O_4 dose, reaction time, Cr (VI) solutions, and the interactions between them required full factorial design when CCD was used to obtain the experimental design matrix. The factors of "n" raise the number of studies for an all copy of the method which is given in Eq. (3):

$$N = 2^n + 2n + n_c \quad (3)$$

Where; 2^n; factorial runs, 2n; axial runs and n_c; center runs. A five-level CCD with four-factor (reaction time, bentonite-Fe_3O_4 dose, pH and chromium concentrations) was used to analyze the effects of parameters. The ranges of the independent changeable were shown in Table 1. The experimental design as suggested by Design Expert Software along with the actual and predicted values were also given in Table 2.

Table 1. All variable factors in CCD

Factors	Term.	Unit	Low	High
pH	A	-	2.0	10.0
Adsorbent dose	B	g	0.05	0.2
Cr (VI) con.	C	mg/L	5	10
Temperature (^oC)	D	^oC	25	45
Reaction time	E	min	5	120

Table 2. RSM matrix, experimental (actual) and predicted values of adsorption efficiency and all variable factors in RSM.

Run	A	B	C	D	E	Actual	Predicted	Run	A	B	C	D	E	Actual	Predicted
1	6	0.125	7.5	35	60	43.14	40.99	26	4.31	0.093	8.5	30	40	43.75	44.38
2	4.3	0.156	6.5	30	85	70.35	69.50	27	2	0.125	7.5	35	60	71.97	64.46
3	4.3	0.156	6.5	40	85	60.13	60.03	28	7.68	0.093	8.5	40	40	16.51	19.93
4	7.6	0.156	8.5	30	40	38.19	41.59	29	6	0.2	7.5	35	60	62.14	60.38
5	4.31	0.093	8.5	40	40	39.19	97.94	30	7.68	0.093	6.5	40	85	39.52	36.61
6	6	0.125	7.5	35	60	43.13	42.77	31	6	0.125	7.5	35	60	43.13	42.77
7	10	0.125	7.5	35	60	16.74	17.88	32	4.31	0.093	6.5	40	40	41.56	40.98
8	6	0.05	7.5	35	60	21.41	18.71	33	7.68	0.093	6.5	30	85	32.53	32.14
9	4.31	0.093	6.5	40	85	51.95	51.69	34	4.31	0.156	8.5	40	40	56.51	55.19
10	7.68	0.156	8.5	40	40	39.73	39.86	35	4.31	0.156	8.5	30	40	58.52	64.07
11	7.68	0.093	8.5	30	85	24.16	27.78	36	4.31	0.156	6.5	30	40	74.32	76.16
12	7.68	0.156	8.5	40	85	37.44	35.67	37	6	0.125	7.5	25	60	30	25.40
13	6	0.125	7.5	35	120	50.98	45.62	38	7.68	0.093	6.5	30	40	24.02	25.24
14	7.68	0.156	6.5	30	40	56.89	53.22	39	4.31	0.156	6.5	40	40	62.18	63.85
15	7.68	0.156	6.5	30	85	45.48	49.93	40	4.31	0.093	8.5	40	85	46.17	45.41
16	4.31	0.093	6.5	30	40	48.55	50.86	41	6	0.125	10	35	60	84.93	80.91
17	7.68	0.156	8.5	40	85	46.30	45.41	42	6	0.125	7.5	35	60	43.13	41.98
18	6	0.125	7.5	35	60	43.13	42.77	43	7.68	0.093	8.5	30	40	25.10	19.22
19	4.31	0.156	8.5	30	85	61.34	59.07	44	6	0.125	7.5	45	60	20	20.14
20	6	0.125	7.5	35	60	43.13	41.98	45	6	0.125	5	35	60	96.84	96.40
21	6	0.125	7.5	35	60	43.13	41.98	46	6	0.125	7.5	35	5	33.93	34.83
22	4.31	0.156	8.5	40	85	54.22	57.36	47	7.68	0.156	8.5	30	85	39.86	39.97
23	7.68	0.156	6.5	40	85	50.42	51.96	48	7.68	0.156	6.5	40	40	53.66	48.06
24	4.31	0.093	6.5	30	85	52.29	54.39	49	4.31	0.093	8.5	30	85	43,48	49.57
25	7.68	0.093	6.5	40	40	19.25	22.52	50	6	0.125	7.5	35	60	43,13	41.98

The relationship between the independent and dependent variables was examined in the CCD by using the second-order polynomial model. The recovery percentage was calculated as shown in Eq. (4):

$$Y = \beta_0 + \sum_{i=1}^{k} \beta_i x_i \sum_{i=1}^{k} \beta_{ii} x_i^2 + \sum_{i=1}^{k} \sum_{j=1}^{k} \beta_{ij} x_i x_j + \varepsilon \tag{4}$$

Where β_o is the offset term; β_i and β_{ii} are the linear and quadratic effects of input factor of X_i; β_{ij} is the linear effect between the independent factor for X_i and X_j; and ε is the error [31].

3. RESULTS

3.1. Characterization of Bentonite-Fe_3O_4 Nanocomposite

SEM surface analyses of the Bentonite-Fe_3O_4 particles before and after the adsorption were used to identify synthesized particles and were shown in Fig. 1(a-d). The Bentonite-Fe_3O_4 was an irregular polyhedron with a rough surface. In order to determine the elemental content of the bentonite-Fe_3O_4 nanocomposite, Energy Dispersive X-Ray (EDX) analysis was carried out and shown in Figure 1(e). In EDX analysis, only a small piece of material is selected from the surface, and can only be examined qualitatively. The EDX spectrum showed that the chemical composition of the nanocomposite produced was mainly composed of iron (50.92 %), oxygen (30.13%), silicon (16.30%), aluminium (2.21%) and chromium 0.44%. According to SEM results, average dimension of Bentonite-Fe_3O_4 nanoparticles was found to be 8.404μm.

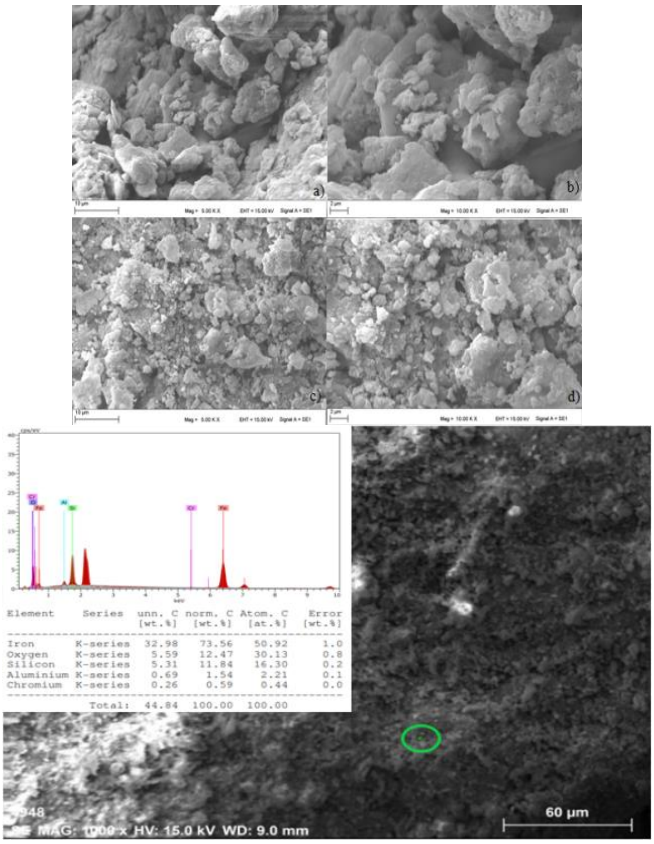

Figure 1. SEM-EDX of raw Bentonite-Fe_3O_4 (a-b) and after adsorption (c-d) with adsorbed Cr(VI)

FTIR analyses were made to compare the surface chemical composition of the materials on which raw Fe_3O_4 produced in this study, and Bentonite-Fe_3O_4 particles (before and after the adsorption), and spectra obtained were shown in Fig. 2. For raw Fe_3O_4 spectrum, the peaks at 1593.15 cm^{-1} and 549.93 cm^{-1} belonged to the C=C stretching and Fe stretching vibrations, respectively. Before the adsorption process, for Bentonite-Fe_3O_4, the peaks at 3010.61 cm^{-1} and 3119.53 cm^{-1} correspond to the stretching vibration of Al-OH, and HO-H. The peaks at 1002.98 cm^{-1}, 919.11 cm^{-1} and 514.70 cm^{-1} belonged to the Si-O stretching, Al-O bending [32] and Fe stretching vibrations [33]. As shown in Fig. 2, the adsorption peaks in the ranges of 514.70 to 1002.98 cm^{-1} and 3332.45 to 2802.19 cm^{-1} were associated with the Fe_3O_4 nanoparticles coated with bentonite.

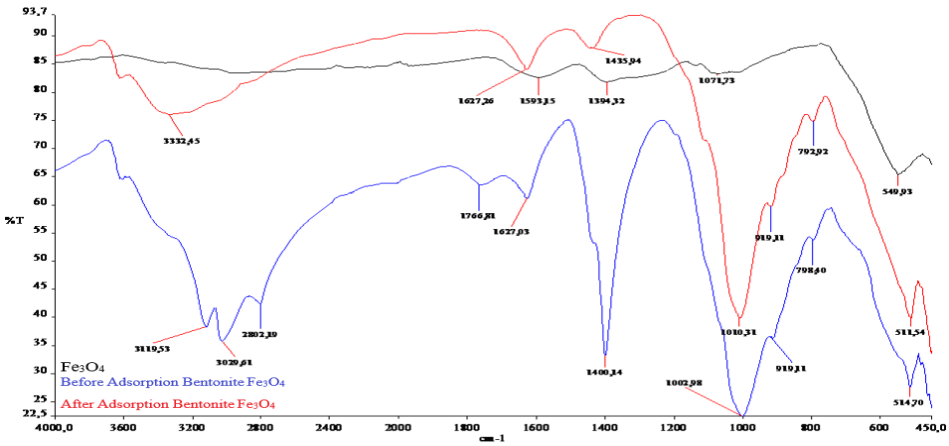

Figure 2. FT-IR spectra of raw Fe_3O_4, and before and after the adsorption of Bentonite-Fe_3O_4

3.2. Adsorption studies

3.2.1. Effect of pH

Based on the speciation diagram of Cr (VI) ions, it is normally present in three main anionic forms of $Cr_2O_7^{2-}$, $HCrO_4^-$ and CrO_4^{2-} which are controlled by the pH of the system and the concentration of these ions in the solution. In an extremely acidic media (pH< 1.0), Cr (VI) is found as alkali H_2CrO_4, and there are basically two basic forms of equilibrium, $Cr_2O_7^{2-}$ and $HCrO_4$ in the $2.0 \leq pH \leq 6.0$ pH range. The general trends for the removal results of Cr(VI) ions reflected a continuous decrease in the percentage of removal efficiency with increasing the pH values from pH 2.0 to 10.0 (Fig. 3a, b, c, d). The removal efficiency increased with increasing of reaction time in the first 60 min, then reached to equilibrium. The maximum Cr (VI) removal efficiency was obtained at pH 2.0 and contact time of 60 min. This result showed that adsorption behavior was favorable under acidic conditions, because there were large amount of H^+ in environment with lower pH value (Fig. 4). Common results in the literature regarding the removal of Cr (VI) ions reveal higher removal efficiency in the acidic medium [32, 34, 35, 36].

3.2.2. Effect of Bentonite-Fe_3O_4 dose

The effect of adsorbent dose on the adsorption process was shown in Fig.3f. The removal of Cr (VI) increased when the adsorbent dosage increased from 0.05 to 2 g/L. This increase may be due to the increase in the total available surface area of the adsorbent particles [37]. In the removal of Cr (VI) ions from water, the adsorption duration to reach equilibrium was found to be 120 min. When the adsorption performances obtained against mixing periods were taken into consideration, the metal ion uptake was found to be higher in the first minutes. Initially, the adsorption rate was higher than the desorption rate. However, with the increasing of mixing time, adsorption and desorption rates were equalized; thus the adsorption balance was established [38]. This result showed the optimum Bentonite-Fe_3O_4 dose was to be 2 g/L (Figures 3b, 3e and 3f).

3.2.3. Effect of Cr (VI) Concentration

The effect of initial Cr (VI) concentration on the adsorption process was illustrated in Fig. 4e. As expected, initial Cr (VI) concentration constantly increased, the reason for the decrease in the

removal efficiency was due to the limitation of the number surface area to be adsorbed [39]. However, Cr (VI) removal efficiency increased with increasing of Bentonite-Fe_3O_4 dose in the solution. Optimum Cr (VI) removal was obtained in the Cr (VI) concentration of 6.5 mg/L (Fig 4c and 4e).

3.2.4. Effect of Temperature

The effect of temperature on the adsorption process was shown in Fig. 4d. It can be seen that the adsorption of Cr (VI) increases when the temperature rases from 25 to 35 °C. It was found that the adsorption efficiency decreased as the temperature continued to increase. With further increasing the adsorption temperature, the adsorption efficiency decreased. The results showed that the optimum temperature was 35 ^{0}C.

3.3. Modeling and statistical analysis

All experiments of this study were created using the Response Surface Method (RSM) on Desing Expert 12 software. Cr (VI) concentration, pH, Bentonite-Fe_3O_4 dose and reaction time in the medium are important for the removing of Cr(VI) from the aqueous solution by using Bentonite-Fe_3O_4 particles. RSM design was used to investigate the combined effects of different parameters on the process. In this study, linear, two-factor interaction (2FI), quadratic and cubic types were used to analyse experimental data to obtain regression equations. The model equation representing efficiency (%) was expressed as functions of pH (A), Bentonite-Fe_3O_4 dose (B), Cr (VI) concentration (C), and temperature (D) for coded units as given below Eq. (5). From Eq. (5), it can be seen that the pH, Bentonite-Fe_3O_4 dose, Cr (VI) concentration, and temperature had a positive effect on the Cr (VI) adsorption. A positive value represents an effect that favors the optimization, while a negative value indicates an inverse relationship between the factor and the response [40].

$$Efficiency\ (\%) = 43.69 - 248.86A + 216.53B + 29.89C\ 14.53E + 6.68AD + 13.52BE + 6.71DE + 238.16C^2 + 45.23D^2 \quad (5)$$

The analysis of variance (ANOVA) was also studied for the determination of the importance of the suggested model (Table 2). The ANOVA results demonstrated that the regression model was highly significant as a large F value and a very low P-value [41]. The model F-value of 42.69 implies the model is significant. There is only a 0.01% chance that an F-value this large could occur due to noise. P-values less than 0.0500 indicate model terms are significant. In this case A, B, C, E, AD, BE, DE, C^2, D^2 are significant model terms. Values greater than 0.1000 indicate the model terms are not significant so the temperature is an insignificant model term. The value of predicted correlation coefficients (R^2:87.46) is reasonable in agreement with the value of adjusted correlation coefficients (R^2:94.57) and the difference is less than 0.2. Adeq Precision measures the signal to moise ratio. A ratio greater than 4 is desired, and the value of this study shows an adequate signal with a ratio of 30.592. The data were also analyzed to check the "actual" and "predicted" model results as shown in Fig. 4. Figure 4 showed that the data was understandably close to a straight line (R^2:0.9457). There with shows that the developed model is sufficient to estimate the experiments response factors since it is distributed close to the "actual axis" (Table 2).

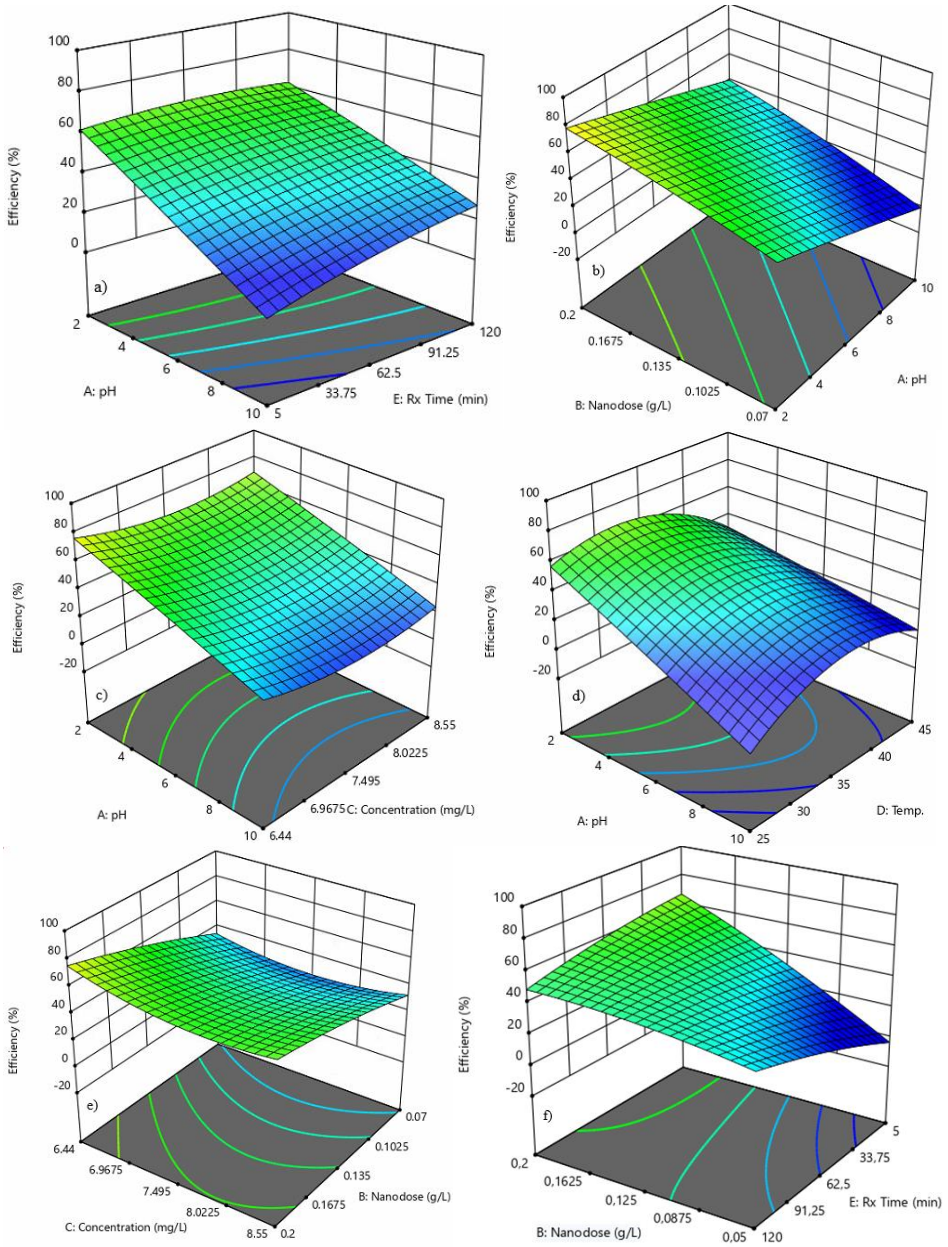

Figure 3. Effect of a) pH-Reaction time on Cr (VI) removal, b) pH-Bentonite-Fe_3O_4 dose on Cr (VI) removal, c) pH-Cr (VI) concentration on Cr (VI) removal, d)pH-Temperature on Cr (VI) removal, e) Cr (VI) Concentration-Bentonite-Fe_3O_4 dose on Cr (VI) removal and f) Bentonite-Fe_3O_4 dose-reaction Time on Cr (VI) removal

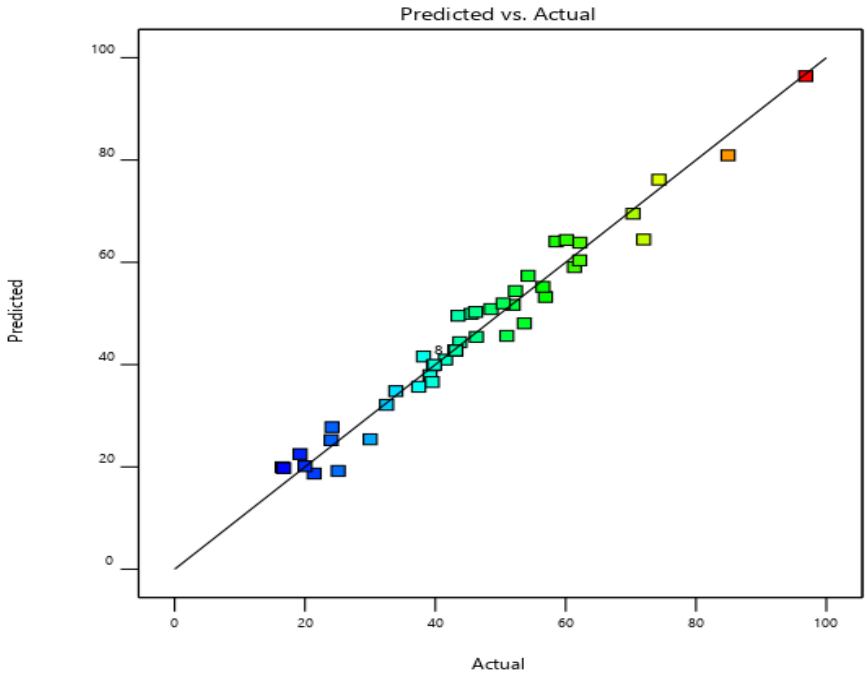

Figure 4. Predicted and actual values for Cr (VI) removal by Bentonite-Fe_3O_4.

Table 3. ANOVA analysis of variance table

Source	SS	Df	MS	F-value	p-value	Source	SS	Df	MS	F-value	p-value
Model	133415.92	20	670.80	43.69	< 0.0001	DE	103.04	1	103.04	6.71	0.0148
A	3821.11	1	3821.11	248.86	< 0.0001	C^2	3656.83	1	3656.83	238.16	<0.0001
B	3324.67	1	3324.67	216.53	< 0.0001	D^2	694.55	1	694.55	45.23	<0.0001
C	458.88	1	458.88	29.89	< 0.0001	R^2	0.9679	Adjusted-R^2		0.9457	
D	52.92	1	52.92	3.45	0.0736	Adeq-Pr	30.5921	Predicted-R^2		0.8746	
E	223.14	1	223.14	14.53	0.0007	SS: Sum of Square, MS: Mean of Suqaure, A: pH, B: Bentonite-Fe_3O_4 Dose, C: Cr (VI) Concen., D:Temp., E:Rx Time, Pr: Precision					
AD	102.58	1	102.58	6.68	0.0150						
BE	207.62	1	207.62	13.52	0.0010						

3.4. Adsorption Isotherms and kinetics

The adsorption isotherms were used to understand how the adsorbed molecules were distributed between the aqueous and solid phases under equilibrium conditions [42]. The experimental data were applied to the Langmiur, Freundlich, Tempkin, and Harkins–Jura isotherm equations. The constant parameters of the isotherm equations for these adsorption process were calculated by regression using linear form of the isotherm equations. The constant parameters and correlation coefficients (R) were summarized in Table 3 and Figure 5 (a,b,c,d). According to Freundlich isotherm, 1/n value obtained for Bentonite-Fe_3O_4 were less than 1 indicating that Cr (VI) could be easily adsorbed onto the Bentonite-Fe_3O_4 surface. The results show that adsorption was more suitable for the Tempkin isotherm model.

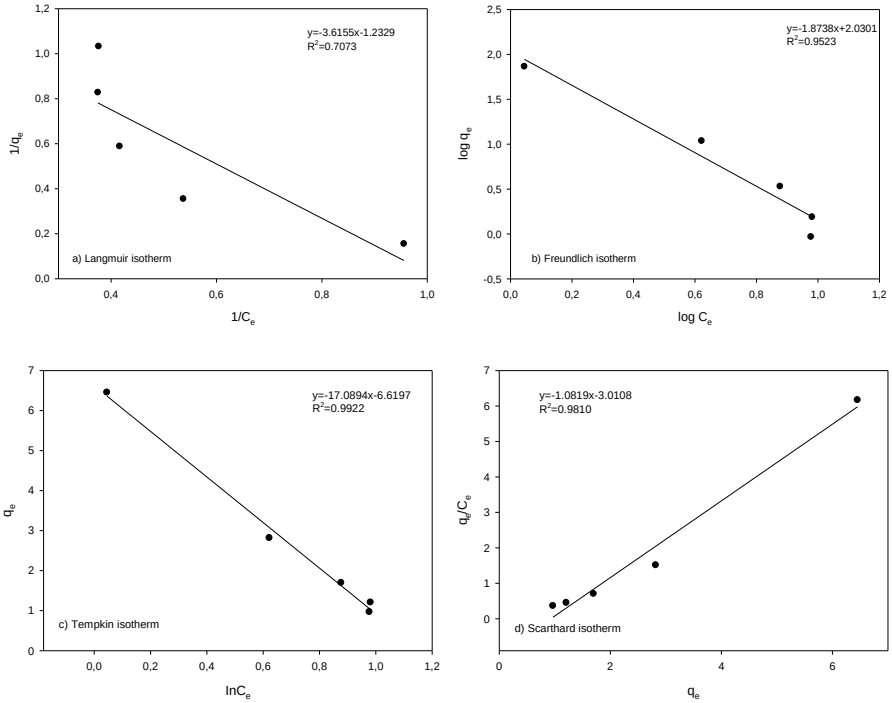

Figure 5. The isotherm modeling results of Cr(VI) adsorption by Bentonite-Fe_3O_4

Table 4. The isotherm models and constants

Langmuir Isotherm Model		**Freundlich Isotherm Model**	
$\frac{1}{q_e} = \frac{1}{bq_mC_e} + \frac{1}{q_m}$		$\ln q_e = \ln K_f + \frac{1}{n}\ln C_e$	
Q (mg/g)	0.28	K_f (mg/g)(L/mg$^{1/n}$)	5.51
b (L/mg)	2.90	n	0.53
R^2	0.7073	R^2	0.9523
Tempkin Isotherm Model		**Scarthcard Isotherm Model**	
$q_e = \frac{R.T}{b_T}.\ \ln(A_T.C_e)$		$\frac{1}{q_e^2} = \left(\frac{B}{A}\right) - \left(\frac{1}{A}\right)\log C_e$	
B_1	17.09	Ks	1.08
K_T (L/g)	0.39	Qs	2.79
R^2	0.9922	R_2	0.9810

q_e: amount adsorbed, b: Langmuir constant, C_e: equilibrium concentration q_m: monolayer adsorption capacity, K_f and n: Freundlich constants, R: constant, T: temperature, b_T and A_T: Tempkin isotherm constant, A and B: Harkins-Jura constants.

Kinetic studies are important for the prediction of optimal terms in the full-scale adsorption mechanism [43]. Kinetic modeling provides useful information about adsorption mechanisms and possible rate-controlling steps [44]. Kinetic constants and correlation values (R^2) were

summarized in Table 4 and Fig. 6. The results showed that adsorption was more suitable for the Pseudo-second-order model, so that chemisorption could be the rate-limiting step.

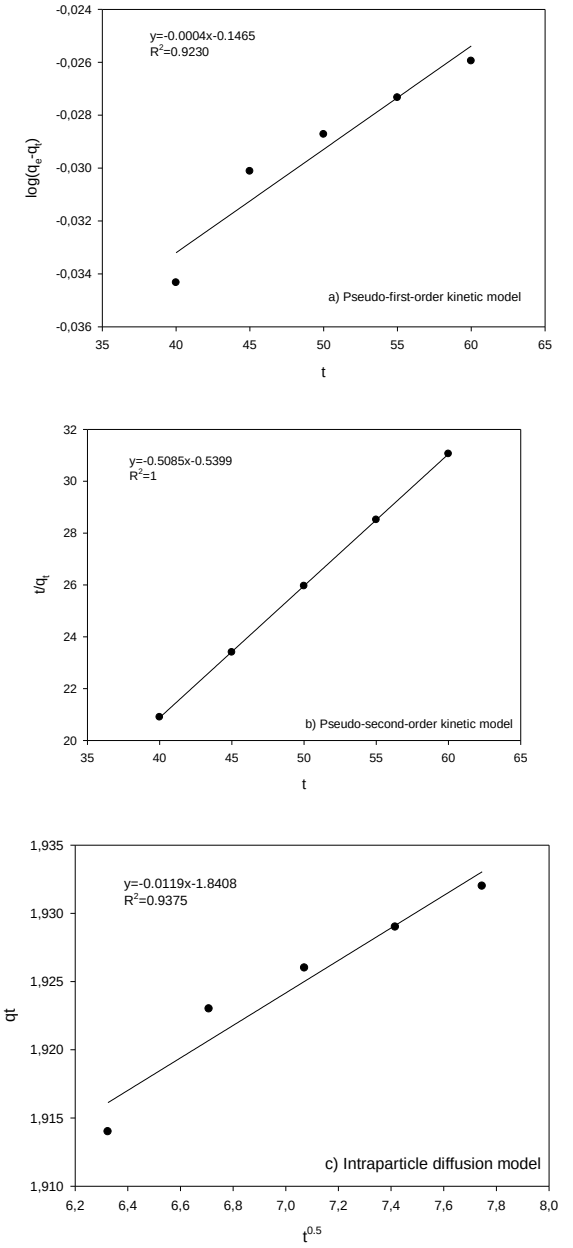

Figure 6. The kinetic modeling results of Cr (VI) adsorption by Bentonite-Fe_3O_4

Table 5. The kinetic models and constants

Pseudo-First Order Kinetic Model			Pseudo-Second Order Kinetic Model			Intraparticle Diffusion Model		
k_1 (l/min)	qe (mg/g)	R^2	k_2 (l/min)	qe (mg/g)	R^2	k_p (g.dk$^{0.5}$)	C (mg/g)	R^2
0.0009	1.92	0.9230	3.7	0.5	1	0.01	1.84	0.9375
$\log(q_e - q_t) = \log q_e - \frac{k_1}{2.303} * t$			$\frac{1}{q_t} = \left[\frac{1}{k_2 * q_e{}^2}\right] + \frac{1}{q_e} * t$			$q_e = k_p t^{0.5} + C$		

k_1: first-order constant, k_2: second-order rate constant, k_p: intra-particle diffusion rate constant, C: boundary layer thickness.

4. CONCLUSION

In the present study magnetite nanocomposites coated with bentonite were successfully synthesized as adsorbent materials. According to the characterization results, Bentonite-Fe_3O_4 had a structure similar to an uneven surface and irregular polyhedron. In ANOVA results, F value (42.69) indicated that the model was significant, and the parameters affecting the adsorption process such as pH, Bentonite-Fe_3O_4 dose and Cr (VI) concentration were important model conditions. RSM was used to investigate the optimum ambient conditions of parameters to remove Cr (VI), and the effects of the square of each parameter were optimally significant with the CCD method. According to the results, optimum adsorption efficiency of Cr (VI) removal (96.84%) was obtained in 7.5 mg/L initial metal ion concentration at contact time of 60 min., pH 2.0, adsorbent dosage of 1.25 g/L and temperature of 35 ^{o}C. Comparing the adsorption efficiency of bentonite-Fe_3O_4 with the previous studies in the literature is important to put forward the importance of adsorbent (Table 6). Table 6 shows that Bentonite-Fe_3O_4 used in this study is a convenient and useful adsorbent for adsorption of Cr (VI) from the aqueous medium. In addition, the advantages include easy separation of bentonite from water, an abundance of bentonite in nature, magnetite part activating bentonite surface area, and short contact time of the adsorption process.

Table 6. Comparison of the maximum efficiency and adsorption capacities of Cr(VI) on various adsorbents

Adsorbent	**Conditions**	**Efficiency (%) / Adsorption Capacity (mg/g)**	**Ref.**
Kaolinite	pH 3.0-10.0 Dose 20 g/L Cr (VI) 5.2 mg/L Time 24 h Temp. 25 ^{0}C	90 %	[45]
Natural Bentonite	pH 1.0-13.0 Dose 0.2 g/L Cr (VI) 10.4- 270 mg/L Time 24 h Temp. 25 ^{0}C	98.46 % 624 mg/g	[46]
Fire Clay	pH 2.0 Dose 2.5 g/50 mL Cr (VI) 2-10 mg/L Time 90 min Temp. 20 ^{0}C	0.11	[47]
Illite	pH 3.0-10.0 Dose 20 Cr (VI) 5.2 mg/L Time 24 h Temp. 25 ^{0}C	60 %	[45]
Kaolin	pH 2.0 Dose 25 g/L Cr (VI) 200 mg/L Time 60 Temp. 25 ^{0}C	0.38	[48]
Poly(tannin-tetrathylenepentamine)	pH 2.0 Dose 50 mg Cr (VI) 200 mg/L Time 48 h Temp. 35 ^{0}C	397.52 mg/g	[49]
Activated carbon coated glass fiber fabric	pH 2.0 Dose 2 g/L Cr (VI) 50 mg/L Time 2 h Temp. 45 ^{0}C	96.54 % 22.62 mg/g	[50]
Chitosan/Bentonite	pH 2.0 Dose 0,25 g Cr (VI) 500 mg/L Time 150 min Temp. 20 ^{0}C	89.13 %	[51]
Bentonite-Fe_3O_4	pH 2.0 Dose 2.5 g/L Cr (VI) 6.5 mg/L Time 60 min Temp. 35 ^{0}C	77.46 %	This Study

REFERENCES

[1] Le A. T., Pung S. Y., Sreekantan S., & Matsuda A., (2019) Mechanisms of removal of heavy metal ions by ZnO particles, *Heliyon*, *5*(4), e01440.

[2] Chen H., Teng Y., Lu S., Wang Y., Wang J., (2015a) Contamination features and health risk of soil heavy metals in China, *Sci. Total Environ.*, 512–513, 143–153.

[3] Byber K., Lison D., Verougstraete V., Dressel H., Hotz P., (2016) Cadmium or cadmium compounds and chronic kidney disease in workers and the general population: a systematic review. Crit. Rev., *Toxicol.*, 46 (3), 191–240.

[4] Wang R., Zhao Y., Xie X., Mohamed T. A., Zhu L., Tang Y., ... & Wei Z. (2020) Role of NH_3 recycling on nitrogen fractions during sludge composting, *Bioresource Technology*, *295*, 122175.

[5] Zhu L., Yang H., Zhao Y., Kang K., Liu Y., He P., Wu Z., Wei Z., (2019) Biochar combined with montmorillonite amendments increase bioavailable organic nitrogen and reduce nitrogen loss during composting, *Bioresour. Technol.* 294, 122224.

[6] Shao N., Li S., Yan F., Su Y., Liu F., & Zhang Z. (2020) An all-in-one strategy for the adsorption of heavy metal ions and photodegradation of organic pollutants using steel slag-derived calcium silicate hydrate, *Journal of hazardous materials*, *382*, 121120.

[7] Gong Y., Zhao D., Wang Q., (2018) An overview of field-scale studies on remediation of soil contaminated with heavy metals and metalloids: Technical progress over the last decade, *Water Res.* 147, 440-60.

[8] Jobby R., Jha P., Yadav A.K., Desai N., (2018) Biosorption and biotransformation of hexavalent chromium Cr(VI): A comprehensive review, *Chemosphere*, 207, 255-66.

[9] Han J.-C., Chen G.-J., Qin L.-P., Mu Y., (2017) Metal respiratory pathway-independent Cr isotope fractionation during Cr(VI) reduction by Shewanella oneidensis MR-1, *Environ. Sci. Technol.* Lett. 4, 500–504.

[10] Ou B., Wang J., Wu Y., Zhao S., & Wang Z., (2020) Efficient removal of Cr (VI) by magnetic and recyclable calcined CoFe-LDH/g-C_3N_4 via the synergy of adsorption and photocatalysis under visible light, *Chemical Engineering Journal*, *380*, 122600.

[11] Sun X., Huang H., Zhu Y., Du Y., Yao L., Jiang X., Gao P., (2019) Adsorption of Pb^{2+} and Cd^{2+} onto Spirulina platensis harvested by polyacrylamide in single and binary solution systems, Colloids Surf. A Physicochem, *Eng. Asp.* 583, 123926.

[12] Liu L., Liu S., Peng H., Yang Z., Zhao L., & Tang A., (2020) Surface charge of mesoporous calcium silicate and its adsorption characteristics for heavy metal ions, *Solid State Sciences*, 106072.

[13] Tan X.L., Fang M., Chen C.L., Yu S.M., Wang X.K., (2008) Counterion effects of Ni^{2+} and sodium dodecylbenzene sulfonate adsorption to multiwalled carbon nanotubes in aqueous solution, *Carbon*, 46 1741–1750.

[14] Tan X.L., Fan Q.H., Wang X.K., Grambow B., (2009) Eu(III) sorption to TiO2 (anatase and rutile): Batch, XPS, and EXAFS study, *Environ. Sci. Technol.*, 43, 3115–3121.

[15] Verma M., Tyagi I., Chandra R., Gupta V.K., (2017) Adsorptive removal of Pb (II) ions from aqueous solution using CuO nanoparticles synthesized by sputtering method, J. *Mol. Liq*., 225, 936–944.

[16] Verma R., Asthan A., Singh A.K., Prasad S., Susan M.A.B.H., (2017) Novel glycine functionalized magnetic nanoparticles entrapped calcium alginate beads for effective removal of lead, *Microchem. J.*, 130, 168–178.

[17] Zhang X., Yan L., Li J., & Yu H. (2019) Adsorption of heavy metals by L-cysteine intercalated layered double hydroxide: Kinetic, isothermal and mechanistic studies, *Journal of Colloid and Interface Science*, 562, 149-158.

[18] Chalermyanont, T. & Arrykul, S. (2005). Compacted Sand-bentonite Mixtures for Hydraulic Containment Liners, Songklanakarin *Journal of Science and Technology*, 27(2), 313-323.

[19] Niu, M., Li, G., Cao, L., Wang, X., & Wang, W. (2020). Preparation of sulphate aluminate cement amended bentonite and its use in heavy metal adsorption, *Journal of Cleaner Production*, 120700.

[20] Kong, S., Wang, Y., Hu, Q., & Olusegun, A. K. (2014). Magnetic nanoscale Fe–Mn binary oxides loaded zeolite for arsenic removal from synthetic groundwater, *Colloids and surfaces A: Physicochemical and engineering aspects*, *457*, 220-227.

[21] Cui, H. J., Cai, J. K., Zhao, H., Yuan, B., Ai, C. L., & Fu, M. L. (2014). Fabrication of magnetic porous Fe–Mn binary oxide nanowires with superior capability for removal of As (III) from water, *Journal of hazardous materials*, *279*, 26-31.

[22] Mehdinia, A., Jebeliyan, M., Kayyal, T. B., & Jabbari, A. (2017). Rattle-type Fe_3O_4@ SnO_2 core-shell nanoparticles for dispersive solid-phase extraction of mercury ions, *Microchimica Acta*, *184*(3), 707-713.

[23] Luo, H., Zhang, S., Li, X., Liu, X., Xu, Q., Liu, J., & Wang, Z. (2017). Tannic acid modified Fe3O4 core–shell nanoparticles for adsorption of Pb^{2+} and Hg^{2+}, *Journal of the Taiwan Institute of Chemical Engineers*, *72*, 163-170.

[24] Tang S.C.N., Lo I.M.C., (2013) Magnetic nanoparticles: essential factors for sustainable environmental applications, *Water Res*., 47, 2613–2632.

[25] Zhan H., Bian Y., Yuan Q., Ren B., Hursthouse A., Zhu G., (2018) Preparation and potential applications of super paramagnetic nano-Fe_3O_4, *Processes*, 6 (4), 33.

[26] Bezerra, M. A., Santelli, R. E., Oliveira, E. P., Villar, L. S., & Escaleira, L. A., (2008) Response surface methodology (RSM) as a tool for optimization in analytical chemistry, *Talanta*, 76(5), 965-977.

[27] Ecer, Ü. and Sahan, T., (2018) A response surface approach for optimization of Pb(II) biosorption conditions from aqueous environment with Polyporussquamosus fungi as a new biosorbent and kinetic, equilibrium and thermodynamic studies, *Desalin. Water Treat.*, 102, 229-240.

[28] Taheri, M., Moghaddam, M.R.A. and Arami, M. (2012) Optimization of acid black 172 decolorization by electrocoagulation using response surface methodology, *Iranian J.Environ.HealthSci.Eng.*, 9 (1), 23-31.

[29] Wang C., Yang, Y., Hou J., Wang P., Miao L., Wang X., & Guo L. (2020) Optimization of cyanobacterial harvesting and extracellular organic matter removal utilizing magnetic nanoparticles and response surface methodology: A comparative study, *Algal Research*, 45, 101756.

[30] Petcharoen, K., & Sirivat, A. (2012). Synthesis and characterization of magnetite nanoparticles via the chemical co-precipitation method.*Materials Science and Engineering: B*, *177*(5), 421-427.

[31] Roosta M., Ghaedi M., Daneshfar A., and Sahraei R., (2014) Experimental design based response surface methodology optimization of ultrasonic assisted adsorption of safaranin O by tin sulfide nanoparticle loaded on activated carbon, *Spectrochimica Acta Part A: Molecular and Biomolecular Spectroscopy*, 122, 223-231.

[32] Abukhadra M.R., Adlii A., & Bakry B.M., (2019) Green fabrication of bentonite/chitosan@ cobalt oxide composite (BE/CH@ Co) of enhanced adsorption and advanced oxidation removal of Congo red dye and Cr (VI) from water, *International journal of biological macromolecules*, 126, 402-413.

[33] Cornell, R.M., Schwertmann, U., (2003) The Iron Oxides: Structure, Properties, Reactions, Occurrence and Uses, second ed., Wiley–VCH, Weinheim.

[34] Ansari R., (2006) Application of polyaniline and its composites for adsorption/recovery of chromium (VI) from aqueous solutions, *Acta Chimica Slovenica*, 53, 88-94.

[35] Liang H., Song B., Peng P., Jiao G., Yan X., & She D., (2019) Preparation of three-dimensional honeycomb carbon materials and their adsorption of Cr (VI), *Chemical Engineering Journal*, 367, 9-16.

[36] Cherdchoo W., Nithettham S., & Charoenpanich J., (2019) Removal of Cr (VI) from synthetic wastewater by adsorption onto coffee ground and mixed waste tea, *Chemosphere*, 221, 758-767.

[37] Xiong J.B., Islam E., Yue M., Wang W.F., (2011) Phosphate removal from solution using powdered freshwater mussel shells, *Desalination*, 276, 2-3, 317–321.

[38] Sun, Y., Yang, S., Chen, Y., Ding, C., Cheng, W., & Wang, X. (2015). Adsorption and desorption of U (VI) on functionalized graphene oxides: a combined experimental and theoretical study, *Environmental science & technology*, *49*(7), 4255-4262.

[39] Owalude S.O., Tella A.C., (2016) Removal of hexavalent chromium from aqueous solutions by adsorption on modified groundnut hull, *Beni-Suef University Journal of Basic and Applied Science*, 5, 377-388.

[40] Mourabet, M., El Rhilassi, A., El Boujaady, H., Bennani-Ziatni, M., & Taitai, A. (2017). Use of response surface methodology for optimization of fluoride adsorption in an aqueous solution by Brushite, *Arabian Journal of Chemistry*, *10*, S3292-S3302.

[41] Srivastava, V., Sharma, Y. C., & Sillanpää, M. (2015). Response surface methodological approach for the optimization of adsorption process in the removal of Cr (VI) ions by $Cu_2(OH)_2CO_3$ nanoparticles, *Applied Surface Science*, *326*, 257-270.

[42] Gholizadeh, A., Kermani, M., Gholami, M., & Farzadkia, M. (2013). Kinetic and isotherm studies of adsorption and biosorption processes in the removal of phenolic compounds from aqueous solutions: comparative study, *Journal of environmental health science and engineering*, *11*(1), 29.

[43] Febrianto J., Kosasih A.N., Sunarso J., Ju Y.-H., Indraswati N., Ismadji S.,(2009) Equilibrium and kinetic studies in adsorption of heavy metals using biosorbent: a summary of recent studies, *Journal of Hazardous Materials*, 162, 616-645.

[44] Park D., Yun Y.-S., Park J.M., (2010) The past, present, and future trends of biosorption, *Bioprocess Engineering*, 15, 86-102.

[45] Veselska, V., Fajgar, R., Čihalova, S., Bolanz, R.M., Gottlicher, J., Steininger, R., Siddique, J.A., Komarek, M., 2016. Chromate adsorption on selected soil minerals: surface complexation modeling coupled with spectroscopic investigation, *J. Hazard. Mater.* 318, 433–442.

[46] Guerra, D., Mello, I., Freitas, L., Resende, R., Silva, R., 2014. Equilibrium, thermodynamic, and kinetic of Cr (VI) adsorption using a modified and unmodified bentonite clay. Int. J. Mining Sci. Technol. 24, 525–535.

[47] Rahmani, A. R., Foroughi, M., Noorimotlagh, Z., & Adabi, S. (2016). Hexavalent chromium adsorption onto fire clay, *Avicenna J Environ Helat Eng*., 3 (1) 5029

[48] Liu, J., Wu, X., Hu, Y., Dai, C., Peng, Q., & Liang, D. (2016). Effects of Cu (II) on the adsorption behaviors of Cr (III) and Cr (VI) onto kaolin, *Journal of Chemistry*, *2016*.

[49] Zhang, Z., Gao, T., Si, S., Liu, Q., Wu, Y., & Zhou, G. (2018). One-pot preparation of P (TA-TEPA)-PAM-RGO ternary composite for high efficient Cr (VI) removal from aqueous solution, *Chemical Engineering Journal*, *343*, 207-216.

[50] Huang, M., Mishra, S. B., & Liu, S. (2017). Waste glass fiber fabric as a support for facile synthesis of microporous carbon to adsorb Cr (VI) from wastewater, *ACS Sustainable Chemistry & Engineering*, *5*(9), 8127-8136.

[51] Liu, Q., Yang, B., Zhang, L., & Huang, R. (2015). Adsorptive removal of Cr (VI) from aqueous solutions by cross-linked chitosan/bentonite composite, *Korean Journal of Chemical Engineering*, *32*(7), 1314-1322.